Protonizable Water Model for Quantum Dynamical Simulations

S. R. Billeter and W. F. van Gunsteren*

Physical Chemistry, ETH Zentrum, CH-8092 Zürich, Switzerland

Received: January 14, 1998

A new functional form for describing proton transfer and hydrogen bond potential energy functions in condensed phase simulations is presented. Rather than fitting a potential energy function to ab initio or experimental potential energy profiles, monopole−dipole interactions are used as proton−protolyte pair potential, and Lennard-Jones functions with variable σ- and ϵ-parameters are used to represent protolyte−proton−protolyte three body interactions. The number of parameters increases linearly with the number of protonizable molecule or molecular fragment types, and only eight parameters are needed per protonizable molecule or molecular fragment type. A parameter set for protonizable SPC/E water is presented, and the results of molecular dynamics (MD) and mixed quantum dynamics (QD)/MD simulations are discussed.

I. Introduction

Proton mobility in water plays an important role in both chemistry and biochemistry, and much work has been devoted to the simulation of proton transfer in water. Various simulation methods have been applied to represent proton transport in water, each of them focusing on different aspects, e.g. Car−Parrinello simulations of liquid water,[1,2] ab initio calculations of protonated water clusters,[3,4] path integral, centroid, or classical molecular dynamics or Monte Carlo simulations using central force fields,[5−7] or empirical valence bond methods[8,9] Analytical expressions for fitting potential energy surfaces to coarse grained data obtained from ab initio calculations of small clusters have been proposed too, both as general methods[4] and as ad hoc sets of functions and parameters.[10] Due to the enormous complexity of proton behavior, none of them can be expected to predict the whole range of phenomena involving proton transport in liquid water and aqueous solutions. The methods, functions, and parameters presented in the current article should be especially suited for simulations in which water is serving as the solvent of protonizable and deprotonizable biomolecules.

Ab initio or other molecular orbital (MO) calculations have been widely used to parametrize force field components such as atomic charges or force constants and equilibrium geometric elements. For obvious reasons, potential energy surfaces fitted to MO energies to obtain reaction profiles have become popular, too. The disadvantages of using such fitted potential energy surfaces for simulations in solution are less obvious than its advantages: First, it is generally inappropriate to use parameters obtained from vacuum calculations for simulating reactions in solution. Applying a reaction field correction is often impossible since the radius of the system changes considerably during the potential energy surface scan. In order to approach a liquid-like behavior, more atoms or molecules should be added to the system for which the energy surface is scanned. The facts that a MO calculation is done at $T = 0$ K and that the minimum energy conformation of a molecular cluster in vacuum can differ essentially from the minimum energy conformation of the same cluster in solution lead to problems in this case: Either very unphysical states are sampled when freezing the relative positions of these atoms to represent the geometry of the solvated cluster or the size of the energy contribution of their relaxation cannot be easily determined. Second, the size of systems which can be calculated within reasonable time using correlated methods and polarizable basis sets is still very limited. The perhaps most severe difficulty is the generalization of a once obtained potential energy surface to other systems and reactions. Using mixed molecular orbital/molecular dynamics ("quantum-classical" simulations), valence bond methods or density functional theory can mitigate the mentioned problems.[11] Considerable progress has been achieved in the past few years.

TABLE 1: Energies and Distances from MP2/6-31G Calculations Used for Parametrizing and Testing the Protonizable SPC/E Water Model**

quantity	system	MP2/6-31G**
$r(H^+-O)$	H^+-H_2O	0.9791 Å
$r(H^+-O)$	$H_2O-H^+-H_2O$	1.1935 Å
$r(H^+-O(H_2O)_1)$	$2H_2O-H^+-H_2O$	1.0377 Å
$r(H^+-O(H_2O)_2)$	$2H_2O-H^+-H_2O$	1.4473 Å
E(system) − E(molecules)	H^+-H_2O	−0.2864 hartree
E(system) − E(molecules)	$H_2O-H^+-H_2O$	−0.3490 hartree
E(system) − E(molecules)	$2H_2O-H^+-H_2O$	−0.3918 hartree

From MP2/6-31G** calculations using Gaussian 92,[12] the protonated water dimer is symmetric with an intermolecular distance of 2.4 Å, while the trimer and the tetramer are built from a hydronium ion and two or three water molecules, respectively (see also Table 1). The intramolecular proton−oxygen distance is 1.0 Å, and its intermolecular pendant is 1.45 Å. Under these circumstances, proton transfers between water molecules in liquid water can be expected to be initiated by the rearrangement of the water molecules in the second and third hydration shell rather than by barrier crossing of the proton, which has been confirmed by quantum calculations using Marcus theory.[13] Therefore, a protonizable water model should reproduce the transition from a flat single-well potential with the global minimum at a 2.4 Å oxygen−oxygen distance to a double-well potential when the oxygen−oxygen distance is increased appropriately. In a preceding article,[10] we have presented a rigid but protonizable water model which is based on the SPC/E water model.[14] The proton potential consisted of proton−water pair interactions and water−proton−water triple interactions whose shapes were both fitted to relaxed MP2/6-31G** potential energy surfaces of the respective clusters in vacuo. The fitted functions used to simulate the protonation

S1089-5639(98)00774-9 CCC: $15.00
Published on Web 05/19/1998

TABLE 2: Model Parameters for One Type of Protonizable Residue or Molecule[a]

symbol	meaning	how to find an initial guess
qm	proton charge times dipole moment	from GROMOS force field
r_{off}	offset distance for monopole−dipole interactions	from molecule diameter
r_0	proton−acceptor distance, protonated state	from GROMOS force field, 1 Å
r_1	proton−acceptor distance, deprotonated state	from GROMOS minimum energy configuration
σ_0	Lennard−Jones distance, proton free	from ab initio minimum distance, vacuum
σ_1	Lennard−Jones distance, proton bound	from σ_0
ϵ_0	Lennard−Jones energy, proton free	from ab initio minimum energy, vacuum
ϵ_1	Lennard−Jones energy, proton bound	from ϵ_0

[a] "Proton bound" means that a proton acceptor other than the oxygen atom of the water molecule under consideration is closer to the proton than the distance r_0 ($s\lambda = 1$).

of a water molecule, solvated by water itself, needed to be continuous over the whole range of proton−water molecule distances: from the bound proton distance until the nonbonded interaction cutoff radius. A distinction between "hydrogen bond" potentials for the solute and electrostatic potentials for solvent molecules was thus not allowed (see ref 10, section 2.6). Energies, distances, and the proton exchange rate could approximately be predicted, but an extra adjustable, system size dependent scaling factor s_{tri} for the three body interactions was required to account for the water−proton−water−water four body interactions. The physical properties and even the stability of the simulations turned out to be very sensitive to the value of that parameter. A continous proton−water pair potential influenced by the positions of other water molecules rather than distinct pair and triple potentials is highly desirable: For a proton bound water molecule pair, the contribution from the three body interaction almost equals the contribution of one proton−water pair, and very slight fitting errors of the three body function for one oxygen being close and the other one far away from the proton are multiplied by the number of oxygen atoms in the sphere containing the far oxygen atom.

In view of this situation we have investigated a new protonizable water model, which contains less parameters and no system size dependent parameter and is easily generalizable to other molecular species. The model has been implemented in the program QDGROMOS[10] and has been tested by mixed quantum dynamics/molecular dynamics (QD/MD) simulations of proton transfer in small water clusters and liquid water.

II. Methods

The underlying physical models and the old, fitted protonizable SPC/E model as well as the quantum dynamics and molecular dynamics program have been described in a preceding article.[10] References to the literature are given there too. The design goals of a new, protonizable SPC/E water model with respect to the existing fitted model are (i) better stability of liquid water simulations, (ii) absence of system size dependent parameters, (iii) less parameters, and (iv) easy generalizability to proton acceptor types other than OH_2 (without the need of fitting to other molecular orbital potential surfaces). The old, fitted protonizable water model consisted of three components: proton−water pair contributions, water−proton−water triple contributions, and an adiabatic polarizability contribution. In the new model, the adiabatic polarizability contribution is the same, while the form and parametrization of the first two contributions were modified. The new model based on Lennard-Jones functions with variable parameters is not aimed at exploring the Grötthus mechanism of proton transfer in water but rather to serve as a protonizable solvent for proteins and other biomolecules, just as the old, fitted model. Table 2 gives an overview of the parameters of the new, variable Lennard-Jones protonizable SPC/E water model.

A. Pair Interactions. As in the old, fitted model, the proton−water pair interactions V_p are written as a sum

$$V_p(r, \alpha, \beta) = V_{rad}(r) + V_{ang}(r, \alpha, \beta) \quad (1)$$

of radial contributions $V_{rad}(r)$ at tetrahedral geometry (of the proton and the water molecule) and angular contributions $V_{ang}(r, \alpha, \beta)$. The proton to oxygen distance is indicated by r, and the angles α and β are defined by the proton, the oxygen atom and one of the hydrogen atoms of the water molecule. The shape of the angular contributions,

$$V_{ang}(r, \alpha, \beta) = \exp\left(-\frac{r}{\rho_{ang}}\right) b_2[(\cos(\alpha) - \cos(\text{tet.}))^2 + (\cos(\beta) - \cos(\text{tet.}))^2] \quad (2)$$

using an exponential decay and the cosine of the tetrahedral angle cos(tet.) has not been modified. The radial contributions are modeled as monopole−dipole interactions in the limit of large proton−molecule distances. The shape of the radial contributions has been chosen to be

$$V_{rad}(r_i) = \frac{qm}{(r_i + r_{off})^2} \quad (3)$$

where qm is the product of the proton charge q and the dipole moment m of the water molecule, r_i is the distance between the proton and the oxygen atom of the water molecule i, and r_{off} is an offset distance to lower the size of the radial pair interactions in the limit of small r_i. The parameter qm does not have to be consistent with charges used in the same simulation: it just has to be of the same order of magnitude. Note that the radial pair interactions do not depend on the orientation of the proton with respect to the water molecule. In the short-distance limit, the angular pair interaction term models the orientation dependence, and in the long-distance limit, an angular correction term could be envisaged as a further improvement of the force field, or the current exponential decay of the angular contributions with the distance could be changed to a $1/r^2$ decay.

B. Three Body Interactions: Variable Lennard-Jones Function. As discussed in ref 10, the proton−water molecule interaction cannot be approximated by a single Lennard-Jones function, since the well of a Lennard-Jones function is much too narrow. Either it is parametrized to represent the hydronium ion, or it can represent the flat, single-well shape of the proton potential for the proton bound water dimer. To resolve this problem, an environment coordinate $s\lambda_i$ for the proton water molecule i pair is introduced, which is zero for a free proton and one for a bound proton (see below). "Free" means that the oxygen atom of no water molecule other than molecule i is closer to the proton than a given hydrogen bond distance (r_1). The interaction

TABLE 3: Elements of the Proton Interaction Pair List (See Section II.D)[a]

symbol	type	dimension	priority	meaning
jpnb	int	max_pnb	1	atom sequence number
jpnbc	int	max_pnb	4	charge group number
ipioxy	int	max_pub	1	index in jpnb of the proton acceptor atom
jpnbt	int	max_pub	4	interaction type
pcg	real	max_pub	1	polarized atom charge
dpcg	real	max_pnb·max_pro	1	polarization charge derivative
prdis	real	max_pnb·max_pro	3	distance atom−proton
prvec	real	3·max_pnb·max_pro	3	vector atom−proton
Iprdis	boole	max_ pnb·max_pro	4	true if within cutoff radius
Icgdis	boole	max_pnb·max_pro	4	true if within polarization cutoff radius
prdmpf	real	max_pnb·max pro	5	damping function of proton-atom interaction
prdmpd	real	max_pnb·max pro	5	damping function derivative
loxy2	boole	max_pnb	4	true if there is a second proton acceptor atom
ipiox2	int	max_pnb	2	if (loxy2), ipioxy of the other acceptor atom
dpcg2	real	max_pnb·max_pro	2	if (loxy2), dpcg with respect to the other acceptor atom
qddis	real	max_pts·max pub	3	distance atom−basis point
qdvec	real	3·max_pts max_pub	3	vector atom−basis point
qdpcg	real	max_pts·max pub	1	polarized charge assuming the basis point's state
qddpcg	real	max_pts·max_pub	1	polarized charge derivative
hf_op	real	3·max_pts·max_pub	1	Hellmann−Feynman operator
qddpc2	real	max_pts·max pub	2	if (loxy2), qddpcg with respect to other acceptor atom
npov	int	max_pro	1	number of overlapping atoms with a proton
jpov	int	max_pov max_pro	1	atom sequence number of overlapping atom
ipiov	int	max_pov·max_pro	1	index in jpnb of the overlapping atom
dcov	real	max_pov·max_pro	1	overlap charge derivative
qddcov	real	max_pts·max_pov	1	overlap charge derivative assuming the basis point's state

[a] The memory consumption for most components is proportional to the maximum number of atoms interacting with the proton, max_pub, and the maximum number of quantum basis functions, max_pts. max_pro is the maximum number of protons, both in the cases of QD and MD. max_pov, the maximum number of atoms overlapping with one proton, is a small number. The priority codes mean unavoidable (1), unavoidable for systems containing molecules other than water (2), considerable CPU time savings (3), code easy to change and small CPU time savings (4), and obsolete (5).

$$V_{lj}(r_i, s\lambda_i) = 4\epsilon(s\lambda_i)[(\sigma(s\lambda_i)/r_i)^{12} - (\sigma(s\lambda_i)/r_i)^6] \quad (4)$$

has two sets of Lennard-Jones parameters, $\{\epsilon_0, \sigma_0\}$ to represent "bonded" proton−water interactions and $\{\epsilon_1, \sigma_1\}$ to represent a hydrogen bond,

$$\epsilon(\lambda) = \epsilon_0 + \lambda\epsilon_1 \quad (5)$$

$$\sigma(\lambda) = \sigma_0 + \lambda\sigma_1 \quad (6)$$

Finally, the parameter $s\lambda_i$,

$$s\lambda_i = \sum_{j \neq i} \lambda_j \quad (7)$$

is defined as the sum of the proton transfer reaction coordinates λ_j,

$$\lambda_j = \begin{cases} 1 & \text{if } r\,(\text{proton} - j) < r_0 \\ 0 & \text{if } r\,(\text{proton} - j) > r_1 \\ {}^1/_4(1 + \cos[\pi(r - r_0)/(r_1 - r_0)])^2 & \text{otherwise} \end{cases} \quad (8)$$

over the oxygen atoms of all water molecules j except molecule i.

C. Adiabatic Polarizability. Despite the problems we mentioned in ref 10, sections 3.1 and 4, the functional form of the adiabatic polarizability of the water molecules, introduced in ref 10, section 2.6.4, eqs 45−61, is used without modification. There are two reasons for keeping the adiabatic polarizability as it is: (i) As already stated in ref 10, section 2.6.4, the GROMOS force field can be used, offering charges for both protonized and deprotonized amino acids and other molecular building blocks. (ii) The results in the current article show that the new polarizable water model is more compatible with the adiabatic polarizability treatment than the previous one. We note that the polarization of a water molecule is more difficult to adequately represent in MD simulations than the polarization of larger molecules or molecular building blocks.

D. Changes in the Implementation. The code for the calculation of the proton potential energy operator has been separated from the GROMOS nonbonded energy calculation, since the proton potential energy may also include perturbed bonded energies if protonized residues other than water are around. In addition, further GROMOS development[15] and QD development can be better coordinated by using a small interface. In the case of a classical representation of the proton, the same code as in case of QD is used with the number of basis points equal to 1. The QD interaction is calculated in four passes: (1) The GROMOS nonbonded interaction pair list is used to find the proton−protonizable residue pairs. For these pairs, a proton interactions pair list is built, the Hellmann−Feynman operator is initialized, the pair interactions are calculated, and the reaction coordinates λ_j are stored for later use. Table 3 lists the elements of the proton interactions pair list. Compared to the version of QDGROMOS described in ref 10, a considerable amount of core memory could be saved by using this pair list, but it is still one of the most memory-consuming parts of QDGROMOS. (2) This pass is reserved for the calculation of electrostatic interactions between protons and atoms that are not part of a protonizable residue. (3) The adiabatic polarization interactions (correction to the unpolarized electrostatic contributions from GROMOS) and the variable Lennard-Jones interactions are calculated here. They both have gradient components to the two partners of the pair and to all other atoms, so that the triples proton−protonizable residue−all atoms have to be considered. (4) The proton−proton electrostatic interactions are calculated. Derivatives with respect to atoms having an electronic overlap contribution in the adiabatic polarizability term (see ref 10, section 2.6.4) are

TABLE 4: Outline of the Variable Time Step Algorithm for the Standard QD/MD Coupling Scheme and the Guessed Leap-Frog Algorithm[10]

loops[a]	action	loops[a]	action
	initiation	$1...n_{step}$, $1...n_{sub}$	QD integration over $\Delta t/n_{sub}$
$1...n_{step}$	calculate interactions	$1...n_{step}$, $1...n_{sub}$	MD integration over $\Delta t/n_{sub}$
$1...n_{step}$	guess Hellmann−Feynman	$1...n_{step}$, $1...n_{sub}$	calculate interactions
$1...n_{step}$	check for exceeded pulse threshold	$1...n_{step}$	calculate observables and write to files
$1...n_{step}$	adjust velocities if required		

[a] n_{step} is the number of time integration steps Δt, and n_{sub} is the number of substeps $\Delta t/n_{sub}$.

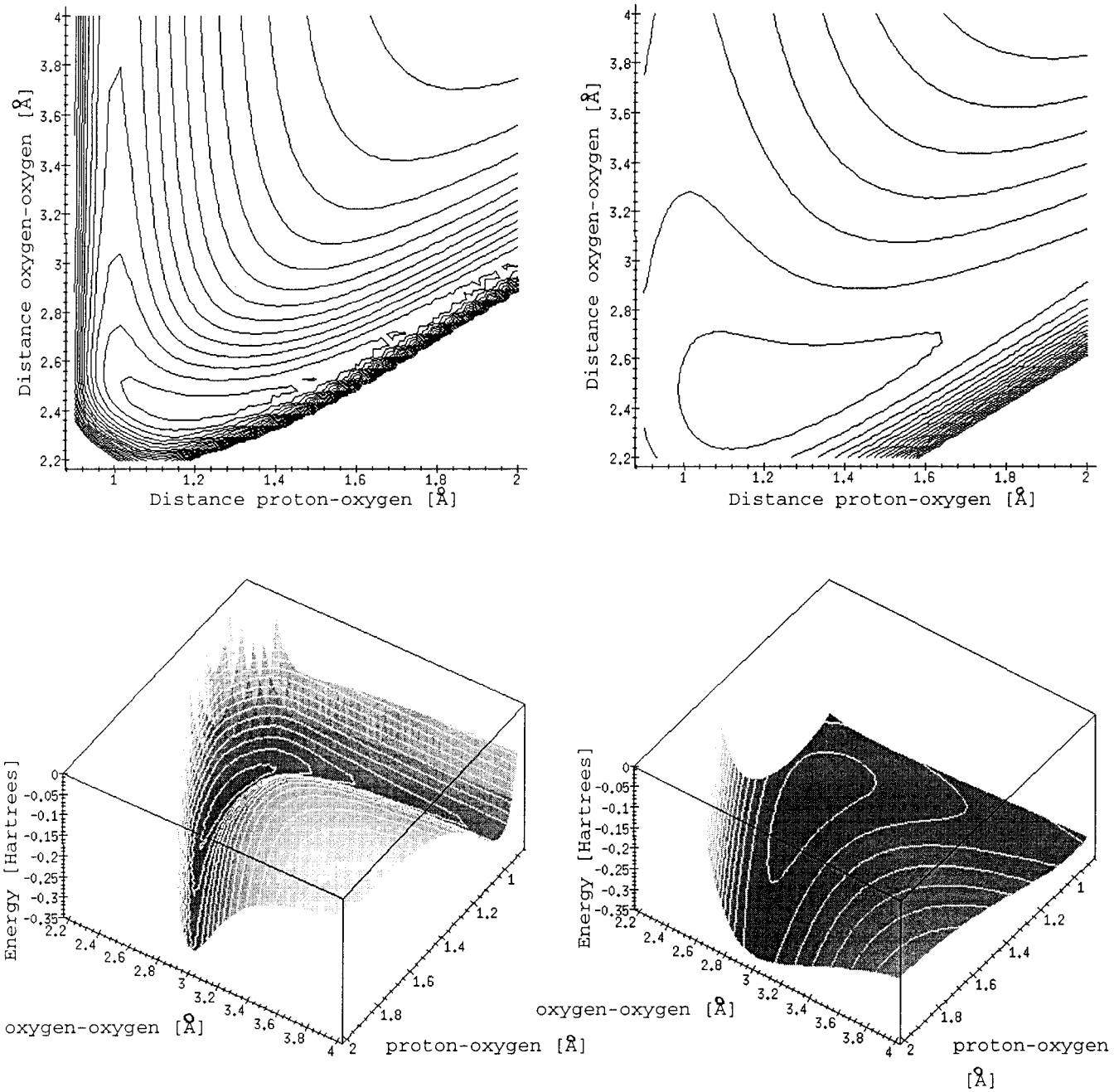

Figure 1. Proton potential energy surfaces for the proton bound water dimer including polarized water−water interactions. Left column: New, variable Lennard−Jones/monopole−dipole functional form. Right column: Old, fitted pair/three body functional form. Top row: Energy contours as function of the proton−oxygen and oxygen−oxygen distances; equidistance, 0.02 hartree. Bottom row: Three-dimensional representation of the potential energy surfaces.

calculated, too. Finally, the potential energy and Hellmann−Feynman operators can be interpolated. Interpolation, however, has not yet been tested.

To increase the much smaller integration time step Δt required by the new protonizable model, a variable time step algorithm has been tried. When the maximum pulse

$$p_{max} = \max_i |F_i| \, \Delta t/n_{sub} \tag{9}$$

F_i being the force (including Hellmann−Feynman forces) to

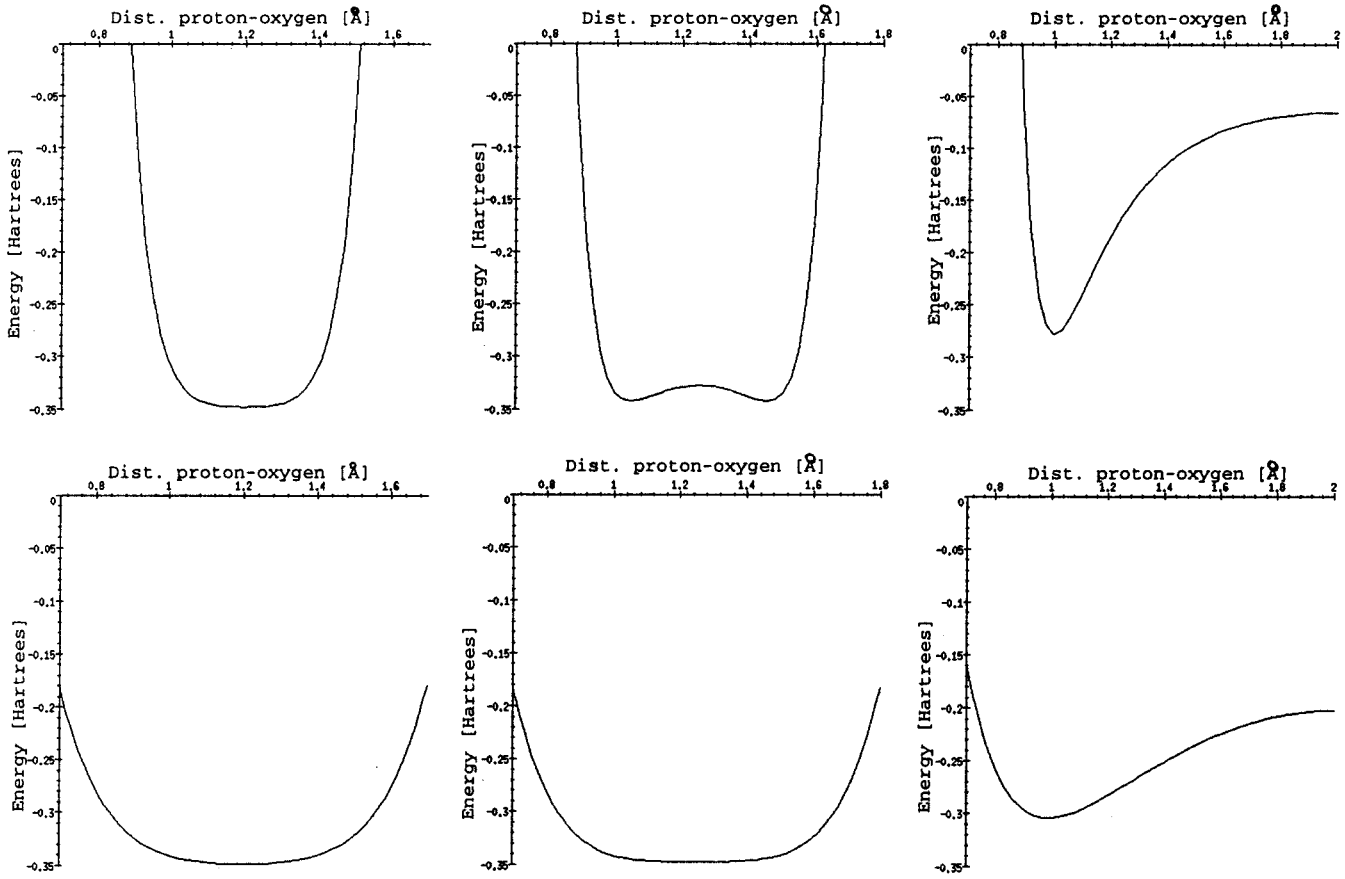

Figure 2. Projection of the potential energy surfaces onto a fixed intermolecular oxygen−oxygen distance r_{OO}: left column, $r_{OO} = 2.4$ Å; middle column, $r_{OO} = 2.5$ Å; right column, $r_{OO} = 4.0$ Å. Top row: New variable Lennard-Jones/monopole−dipole functional form. Bottom row: Old, fitted pair/three body functional form.

atom i and n_{sub} being the number of substeps per time step Δt, exceeds an upper threshold or becomes smaller than a lower threshold value, n_{sub} is multiplied or divided by a factor of 2, respectively. The velocities $V(t - \Delta t/2n_{sub})$ need to be adjusted as well,

$$V(t - \Delta t/2n'_{sub}) = V(t - \Delta t/2n_{sub}) + \frac{\Delta t}{2}\left(\frac{1}{n_{sub}} - \frac{1}{n'_{sub}}\right)F(t) \quad (10)$$

using the forces $F(t)$ and the new number of substeps n'_{sub}. Table 4 outlines the algorithm.

E. Model Systems. When testing the polarizable water model, exactly the same configurations and topologies have been used as in ref 10: the initial configurations of the oligomers have been obtained from MP2/6-31G** calculations carried out using the Gaussian 92 package,[12] and for protonated liquid water, an excess proton has been inserted into a suitable place of an equilibrated box of 216 water molecules. Then, the system has again been equilibrated classically for another 100 ps at 300 K. Periodic boundary conditions of a truncated octahedron and constant volume assuming a density of 1 g/cm^3 have been applied. For the QD simulations, the ground states for the respective water models have been used as initial states. Where extended Hellmann−Feynman forces have been used, the term arising from the change of the occupation numbers has been neglected throughout ("simple extended Hellmann−Feynman forces"; see ref 10, section 2.4).

III. Results

A. Force Field Parameters. Some energies and distances from MP2/6-31G** calculations which can be used for parametrizing and testing the protonizable water models are listed in Table 1. In Figures 1 and 2, the proton potential energy surfaces of the proton bound water dimer resulting from the fitted protonizable SPC/E (fit-PSPC/E) water model[10] and from the new, variable Lennard-Jones/monopole−dipole protonizable SPC/E (LJ-PSPC/E) water model are compared against each other. Both models are qualitatively able to reproduce the minimum and the transition from a flat single-well potential at a 2.4 Å oxygen−oxygen distance to a double-well potential when the oxygen−oxygen distance is increased. While the fit-PSPC/E surface is very flat, allowing large integration time steps, the LJ-PSPC/E model produces large gradients. The oxygen−oxygen distance at which the fit-PSPC/E potential changes from single well to double well is too large. This transition is reproduced well by the LJ-PSPC/E model. The

TABLE 5: Parameter Set[a] for the Protonizable SPC/E Water Model in Addition to the SPC/E Water Model Parameters Which Are Part of the GROMOS 96 Force Field[15]

param	source	value	param	source	value
qm, e^2·Å	LJ-PSPC/E	0.3	ϵ_0, hartree	LJ-PSPC/E	0.180
r_{off}, Å	LJ-PSPC/E	0.4	ϵ_1, hartree	LJ-PSPC/E	0.108
ρ_{ang}, Å	fit-PSPC/E	1.0	q_O^∞, e	fit-PSPC/E	−0.8476
b_2, hartree	fit-PSPC/E	0.280	q_H^∞, e	fit-PSPC/E	0.4238
r_0, Å	LJ-PSPC/E	1.0	$q_{H^+}^\infty$, e	fit-PSPC/E	1.0000
r_1, Å	LJ-PSPC/E	1.8	Δq_{ovl}, e	fit-PSPC/E	18.3923
σ_0, Å	LJ-PSPC/E	0.9	Δq_{pol}, e·Å^2	fit-PSPC/E	0.1562
σ_1, Å	LJ-PSPC/E	1.1	ρ_{ovl}, Å	fit-PSPC/E	0.2646

[a] The parameters for the adiabatic polarization and the angular pair interaction (taken from the old, fitted model[10]) are listed as well and indicated as "fit-PSPC/E" in the "source" column. See also Table 2.

TABLE 6: Energy Conservation in a Microcanonical Simulation as a Function of the Number of Water Molecules (System Size), the Proton Representation (Classical, MD, or Quantum Dynamics, QD), the Number of QD Dimensions N_{dqm}, the Number of Grid Points along One QD Dimension N_{ptd}, the Calculation of the Quantum Forces (Standard Hellmann−Feynman, m_ext = 0, or Simple Extended Hellmann−Feynman, m_ext = 1), the Integration Time Step Δt (fs), and the Model Used (Fitted Protonizable SPC/E, "Fitted", or Variable Lennard−Jones Protonizable SPC/E, "LJ")[a]

syst size	N_{dqm}	N_{ptd}	m_ext	Δt	model	$E_{tot.}$(10ps)	$\sigma(E_{tot.}$, 1ps)	$\sigma(E_{tot.}$, 10ps)	$E_{pot.}$(10ps)	$\sigma(E_{pot.}$1ps)	$\sigma(E_{pot.}$10ps)
2		MD		1	fitted	−904.42	1.24	0.86	−956.88	3.77	13.48
2		MD		0.25	LJ	−897.77	0.029	0.43	−906.34	2.75	2.70
2	1	64	0	1	fitted	−902.14	1.77	2.57	−914.07	3.91	3.00
2	1	64	1	1	fitted	−890.77	1.91	3.67	−909.41	4.37	4.95
2	1	64	0	0.16	LJ	−871.22	0.61	22.22	−899.17	2.74	8.10
2	1	64	0	0.20	LJ	−857.26	0.61	33.82	−894.81	2.69	11.43
2	1	64	0	0.25	LJ	−837.68	0.58	48.43	−888.51	2.63	15.96
2	1	64	0	0.30	LJ	−786.03	0.51	97.84	−871.48	2.58	32.74
2	1	64	1	0.25	LJ	−887.53	0.15	1.20	−903.37	4.31	3.84
2	3	10	0	1	fitted	−879.62	1.63	1.53	−901.54	4.93	4.00
3		MD		1	fitted	−1062.00	3.26	1.67	−1085.79	8.72	6.71
3		MD		0.25	LJ	−965.53	0.064	1.01	−990.43	6.32	6.55
3	1	64	0	1	fitted	−1013.30	2.12	25.46	−1083.01	6.47	6.38
3	1	64	1	1	fitted	−980.50	3.89	42.04	−1073.47	7.52	9.30
3	1	64	0	0.25	LJ	−849.29	2.37	100.36	−956.41	7.59	34.31
3	1	64	1	0.25	LJ	−854.61	5.67	28.47	−956.88	9.30	13.48
3	3	10	0	1	fitted	−501.00	4.36	377.59	−816.13	4.80	219.36

[a] For the quantum dynamics calculations, the guessed leap-frog algorithm has been used throughout.[10] The total energy $E_{tot.}$(10ps), averaged over the last 9 ps of a simulation period of 10 ps, and its standard deviations $\sigma(E_{tot.}$,1ps) (over the last 0.5 ps from a 1 ps simulation) and $\sigma(E_{tot.}$, 10ps) (over the last 9 ps from a 10 ps simulation) in brackets, are reported in kilojoules per mole. The potential energy $E_{pot.}$ is reported too.

TABLE 7: User CPU Time (s) Required for One MD or QD/MD Integration Time Step on a DEC Alpha, 266 MHz Workstation for the Old, Fitted Protonizable SPC/E Water Model (Fitted) and the New, Variable Lennard-Jones Protonizable SPC/E Water Model (LJ) as a Function of the Simulation Parameters[a]

				user CPU	
syst size	N_{dqm}	N_{ptd}	propagator	fitted	LJ
2			MD	0.00021	0.00036
2	1	64	EE	0.033	0.030
2	3	8	CH	1.9	1.8
2	3	10	CH	3.8	3.7
2	3	10	EE		106.7
216			MD	0.31	0.51
216	1	64	EE	3.1	3.5
216	3	8	CH	45.4	27.8
216	3	10	CH	90.4	59.2
216	3	10	EE	455.7	218.1

[a] The quantum dynamics simulations have been carried out using the guessed leap-frog algorithm[10] and standard Hellmann−Feynman forces. The Hamilton matrix was not diagonalized at each step if the Chebysheff series expansion (CH) was used as propagator instead of the eigenstate expansion (EE).[17] See also Table 6.

number of model parameters has been reduced from 23 to 16, none of which depends on the system size. The model parameters of the LJ-PSPC/E model are listed in Table 5.

B. Protonated Small Water Clusters. As in ref 10, the required integration time step Δt has been found using microcanonical simulations of small protonated clusters. Considering the results of Table 6, Δt has been chosen to be 0.25 fs, four times smaller than the time step allowed by the fit-PSPC/E model. The required CPU times per MD time step on a DEC Alpha, 266 MHz workstation are listed in Table 7. Due to the more CPU- and memory-effective proton interaction pair list, the CPU time per MD step could be reduced for large systems and basis sets. The variable time step algorithm (section II D) did not allow for a considerable increase of the time step, but it enlarged the noise in the total energy indeed, probably due to the broken time symmetry. As when using the fit-PSPC/E model, the total energy fluctuations in the one-dimensional QD simulations of the trimer are much larger than the values for the dimer due to the violation of conservation of the angular momentum when applying the correctional forces of eq 32 in ref 10, which ensure momentum conservation. Generally, the total energy has been better conserved using the new model than with the old model. Table 8 shows that the geometry and number of proton exchanges are comparable for the two models.

C. Protonated Liquid Water and Quantum Effects. Figure 3 shows the distances from the proton to the six nearest oxygen atoms in liquid water versus time for both models, and

TABLE 8: Proton−Oxygen Distances ($\{r_i\}$, nm) Averaged over the Last 9 ps of 10 ps Simulations and Number of Proton Exchanges (trsfs) during the Same Time Interval[a]

			fitted		LJ	
syst size	N_{dqm}	N_{ptd}	$\{r_i\}$	trsfs	$\{r_i\}$	trsfs
2	MD		0.1177/0.1277	577	0.1159/0.1254	705
2	1	64	0.1204/0.1288	1056	0.1213/0.1245	2125
2	3	10	0.1239/0.1250	657		
3	MD		0.1081/0.1341/0.3055	172	0.1086/0.1371/0.3016	74
3	1	64	0.1147/0.1309/0.3035	1112	0.1168/0.1268/0.3321	1529
3	3	10	0.1234/0.1317/0.2991	325		
4	MD		0.0988/0.1425/0.2575/0.2819	12	0.1036/0.1455/0.2849/0.3036	0
4	1	64			0.1166/0.1286/0.3157/0.3320	1734

[a] A time step of 0.25 fs has been used for the simulations involving the new, variable Lennard-Jones protonizable SPC/E model, and a time step of 1 fs has been used for the simulations involving the old, fitted protonizable SPC/E model. Simple extended Hellmann−Feynman forces have been used. For the fitted model simulations, the three body scaling factor s_{tri} was 1.0, 0.7, and 0.4 for the dimer, trimer, and tetramer, respectively. The root mean square deviations of all reported distances were within the range from 0.003 to 0.004 nm. See also Table 6.

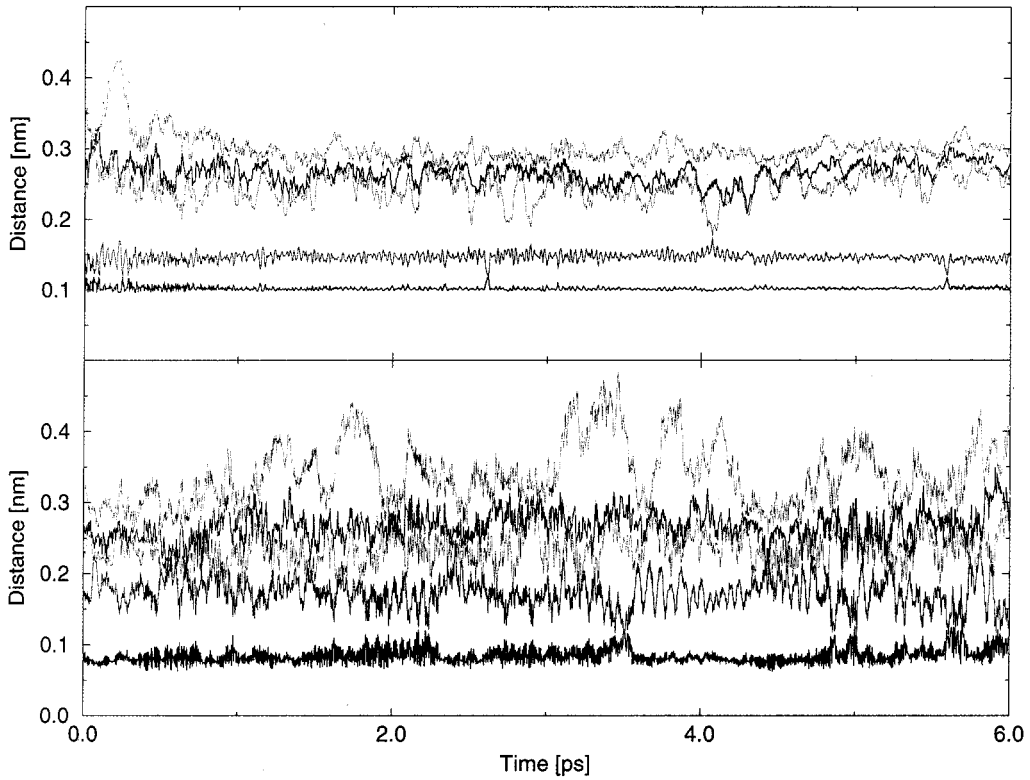

Figure 3. Trajectories of the distances from the excess proton to the six nearest oxygen atoms in protonated liquid SPC/E water at 300 K, over 6 ps using classical molecular dynamics. The integration time step Δt was 0.3 fs. Top: New, variable Lennard-Jones/monopole−dipole functional form. Bottom: Old, fitted pair/three body functions.

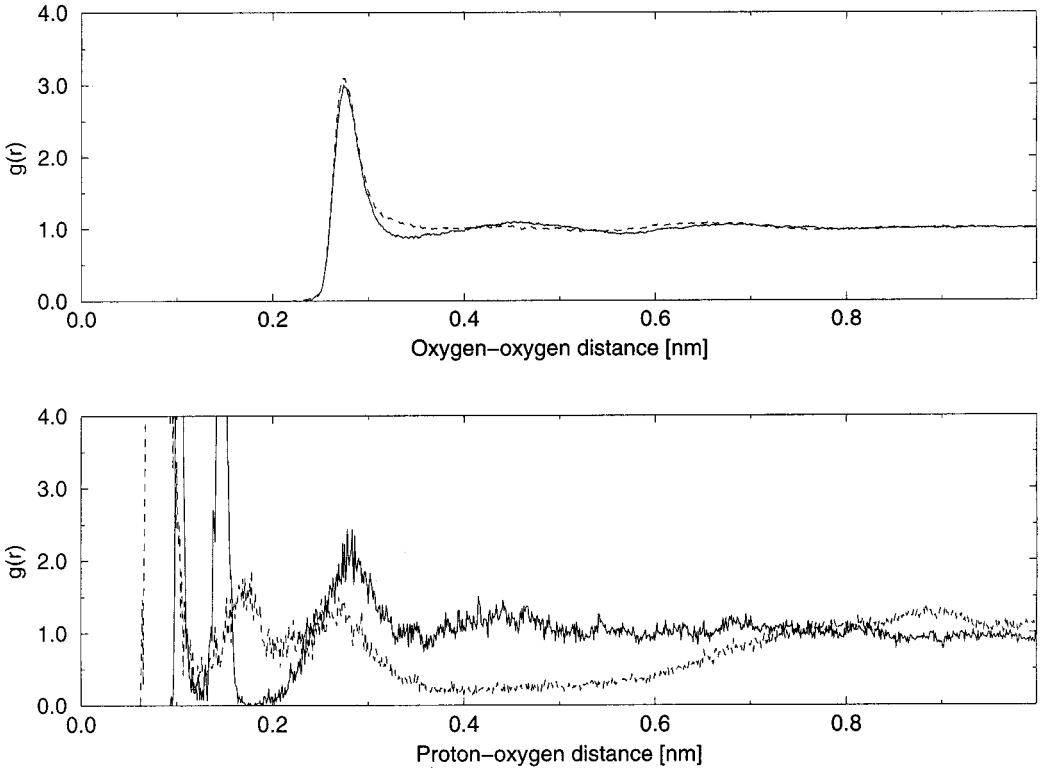

Figure 4. Radial distribution functions of protonated liquid SPC/E water at 300 K, averaged over 6 ps using the variable Lennard-Jones proton potential energy functions (solid line) and using the fitted potential energy functions (dashed line). See Figure 3. Top: Oxygen−oxygen distribution functions. Bottom: Proton−oxygen distribution functions.

Table 9 lists the average distances together with the potential energy and the number of proton exchanges between neighboring oxygen atoms. From the total energies of protonated liquid water over the last 9 ps of 10 ps using the new LJ-PSPC/E model (−10 198.34 kJ/mol classically and −10 200.74 kJ/mol quantum dynamically) and the total energy of pure water over the same period (−8325.26 kJ/mol), the hydration energy of a proton is estimated to be −1873.08 kJ/mol classically and −1875.48 kJ/mol quantum dynamically, compared to −575.62 kJ/mol classically,[10] using the fit-PSPC/E model. From NMR

TABLE 9: Potential Energy $E_{pot.}$ and Its Standard Deviation (in Brackets) and Total Energy $E_{tot.}$ in kilojoules per mole, Distances from the Proton to the Three Nearest Oxygen Atoms $\{r_i\}$ in nanometers, and the Number of Proton Exchanges between Water Molecules (trsfs) of a Protonated System Containing 216 Water Molecules Using Periodic Boundary Conditions of a Truncated Octahedron with an Edge Length of 2.3467 nm[a]

N_{dqm}	N_{ptd}	m_ext	force field	$E_{pot.}$ (1 ps)	$E_{pot.}$ (10 ps)	$E_{tot.}$ (10 ps)	$\{r_i\}$	trsfs
	MD		MD/pure	−9 967.57 (48.12)	−9 967.41 (66.85)	−8 325.26		
	MD		fitted	−11 420.47 (66.37)	−11 163.63 (131.89)	−9 334.67	0.0803/0.1792/0.2337	20
	MD		LJ	−11 694.54 (65.30)	−11 866.86 (69.25)	−10 198.34	0.1022/0.1466/0.2616	2
1	64	1	fitted	−10 122.73 (439.05)	−8 234.51 (438.05)	−4 486.51	0.0921/0.1799/0.2484	84
1	64	1	LJ	−11 732.00 (46.84)	−11 905.87 (93.72)	−10 200.74	0.1165/0.1271/0.2688	1491

[a] The standard deviation of the total energies is not given since the velocities have been scaled to keep the temperature constant. Values from some QD and MD simulations using the variable Lennard-Jones protonizable SPC/E model (LJ) are compared against corresponding values using the fitted protonizable SPC/E model and against values from a simulation of pure, unprotonated SPC/E water (MD/pure). The three body interaction scaling factor for the fitted protonizable SPC/E model was $s_{tri} = 0.27$. For the potential energy $E_{pot.}$ (1 ps), the potential energy was averaged over the last 0.5 ps of 1 ps, and for all other values, it was averaged over the last 9 ps of a 10 ps simulation. See also Tables 6 and 8.

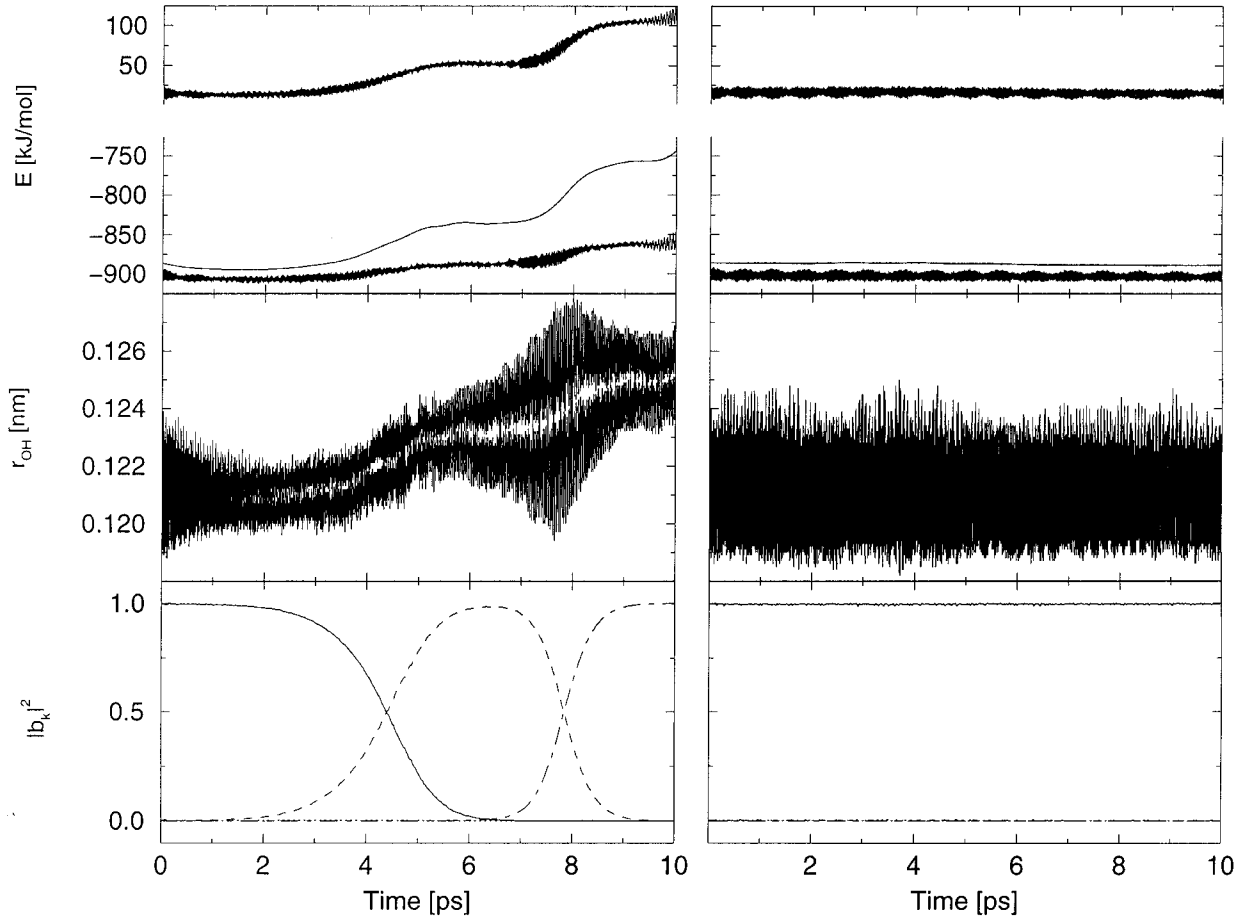

Figure 5. Effect of using standard Hellmann−Feynman forces (left column) or (simple) extended Hellmann−Feynman forces (right column) for the proton bound water dimer in one quantum dimension, 64 basis functions: trajectories over 10 ps using a time step of 0.25 fs and the guessed leap-frog algorithm. Top: Kinetic (top line), total (middle line), and potential (bottom line) energies. Middle: Distance from the proton to the two oxygen atoms. Bottom: Occupation numbers of the ground state (solid line), the first excited state (dotted line), the second excited state (dashed line), and the sum of the occupation numbers of all higher excited states (short−long dashed line). See also Figure 6.

hydrogen exchange data,[16] the second-order positive prototropic charge transfer rate constant of pure liquid water was obtained at 28.0 °C. Transformation into a proton exchange time for the density of 1 g/cm^3 yields 2.5 ps.[10] Mean lifetimes below 1 ps are predicted for the hydronium ion using the one-site prototropic charge migration model, depending on the dynamic pair correlation.[17] This is roughly equivalent to 4 proton transfers per 10 ps, which can be compared to the simulated number of transfers given in Table 9. The number of proton transfers in the first hydration shell of the proton has not changed essentially, but denser surrounding shells result from the new model. The comparison of the radial distribution functions from the excess proton to the oxygen atoms in Figure 4 shows that the LJ-PSPC/E model reproduces these hydration shells more appropriately. The oxygen−oxygen radial distribution functions show slightly more structure for the new model, too. While the liquid protonated water simulations using the fit-PSPC/E model in one quantum dimension had a tendency to crash when using inappropriate parameters due to the (positive) proton coming too close to a (negative) oxygen atom, the corresponding LJ-PSPC/E simulations turned out to be more stable. Since treating the proton quantum dynamically in only one dimension has a number of disadvantages,[10] three-dimensional simulations would be preferred, but such a treatment is very costly. Tables 8 and 9 show that the difference between quantum dynamical (QD) and classical dynamical (MD) proton transfers is consider-

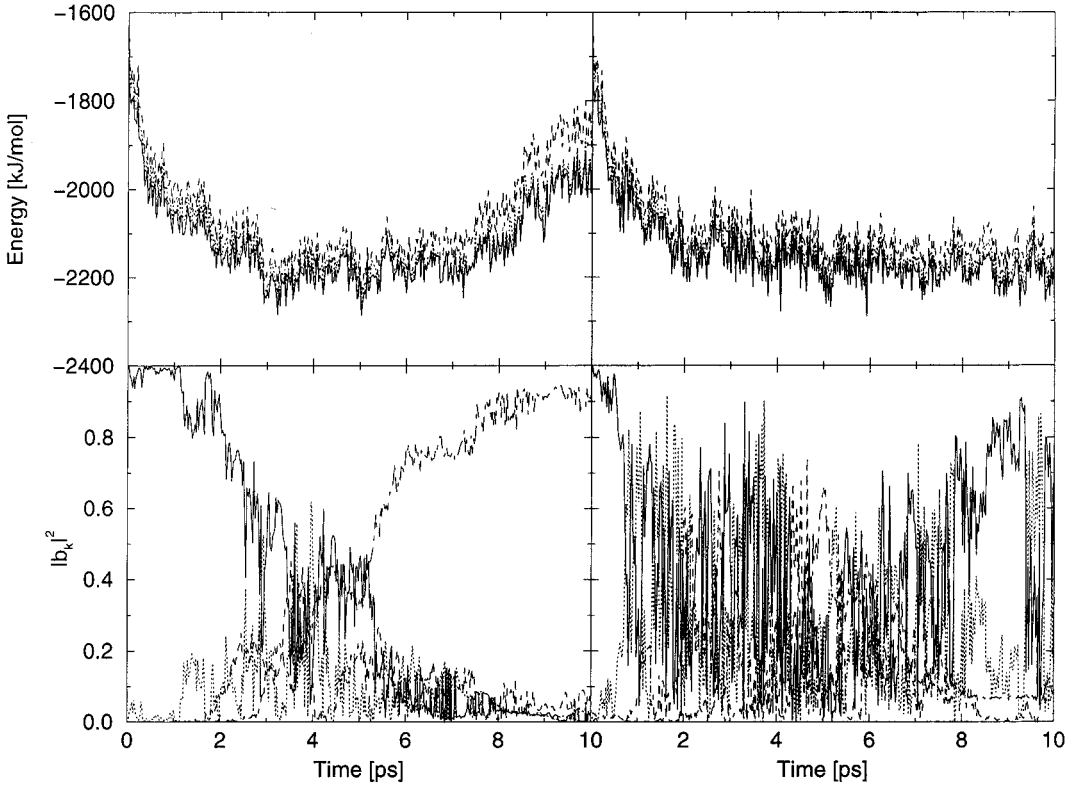

Figure 6. Effect of the use of standard Hellmann−Feynman forces (left side) or (simple) extended Hellmann−Feynman forces (right side) for protonated liquid water, 216 water molecules, in one quantum dimension, 64 basis functions: trajectories over 10 ps using a time step of 0.25 fs and the guessed leap-frog algorithm. Top: Adiabatic energies of the proton ground state (solid line), the first excited state (dotted line), and the second excited state (dashed line). Bottom: Occupation numbers of the ground (solid line), the first excited (dotted line), and the second excited (short dashed line) states and the sum of the occupation numbers of all higher excited states (short−long dashed line). See also Figure 5.

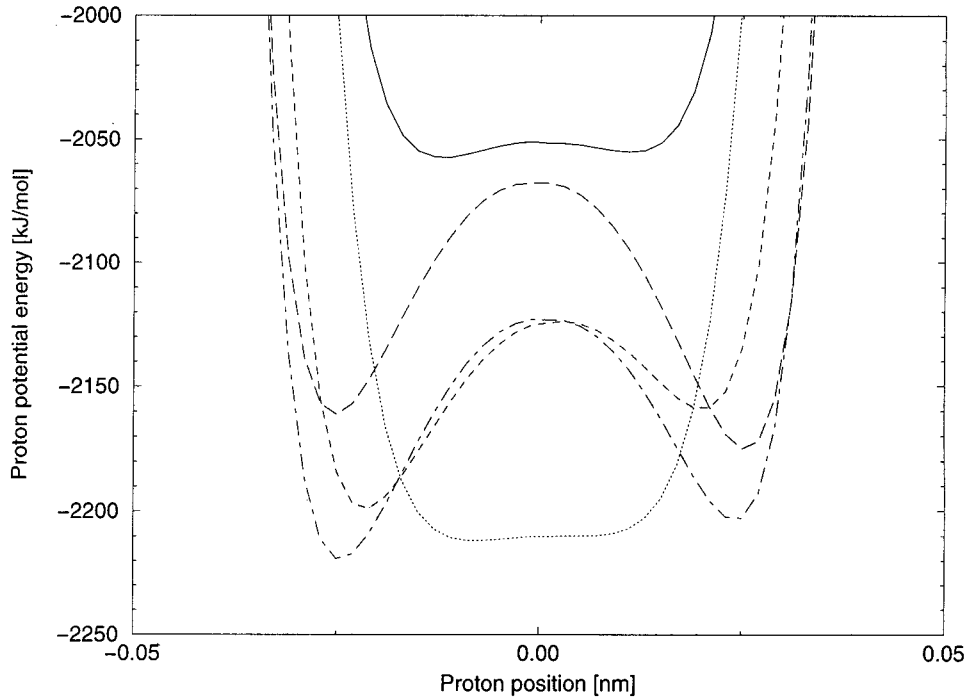

Figure 7. Proton potential energy functions in kilojoules per mole including polarization contributions to the water−water electrostatics for the same system as in Figure 6. Snapshots at 1 ps (solid line), 2 ps (dotted line), 3 ps (short dashed line), 4 ps (long dashed line), and 5 ps (short−long dashed line) have been taken. See also Figure 6 and Table 9.

able. The difference between the number of QD proton transfers and the number of MD proton transfers of the same system under the same conditions can be seen as the effect of tunneling and the presence of excited states. Figures 5 and 6 show trajectories of the occupation numbers of some adiabatic proton states and related properties for the protonated water dimer and for protonated liquid water. Considering the average first proton excitation energy in the liquid case of 20.0 kJ/mol, the occupation number of the lower excited states and the barrier heights from Figure 7, transition involving an excited state is

much more likely than tunneling. From the occupation numbers of adiabatic proton states it is clear that the use of Hellmann−Feynman forces is inappropriate for nonadiabatic QD/MD simulations. The diagonalization of the Hamilton operator is therefore unavoidable even for large systems, and the eigenstate evolution method[18] is the propagation method of choice.

IV. Conclusions and Outlook

An improved protonizable SPC/E water model has been presented and tested. It consists of monopole−dipole and variable parameter Lennard-Jones interaction terms rather than a function fitted to molecular orbital surfaces. Stability problems in liquid water simulations have disappeared and, in contrast to the old model, the generalization to other protonizable residue types such as amino acids is straightforward. These advantages come at the expense of a four times smaller integration time step of 0.25 fs. In addition, three unintended improvements have been observed: (i) The structure of protonated liquid water was better reproduced. (ii) The energy fluctuations in microcanonical simulations were smaller. (iii) Surprisingly, the problems related to the treatment of adiabatic polarizability in the fit-PSPC/E model observed in ref 10 were reduced, although the treatment of the adiabatic polarizability has not been modified. It has been demonstrated that the use of Hellmann−Feynman forces is inappropriate for nonadiabatic mixed quantum dynamics/molecular dynamics simulations. Further work aimed at increasing the integration time step and reducing the CPU time of the calculation of the proton potential energy operator has to be done.

References and Notes

(1) Laasonen, K.; Sprik, M.; Parrinello, M. *J. Chem. Phys.* **1993**, *99*, 9080.
(2) Tuckerman, M. E.; Laasonen, K.; Sprik, M.; Parrinello, M. *J. Chem. Phys.* **1995**, *103*, 150.
(3) Lee, E. P. F.; Dyke, L. M. *Mol. Phys*. **1991**, *73*, 375.
(4) Minichino, C.; Voth, G. A. *J. Phys. Chem. B* **1997**, *101*, 4544.
(5) Halley, J. W.; Rustad, J. R. *J. Chem. Phys.* **1993**, *98*, 4110.
(6) Duh, D.-M.; Perera, D. N.; Haymet, A. D. J. *J. Chem. Phys.* **1995**, *102*, 3736.
(7) Stillinger, F. H.; David, C. W. *J. Chem. Phys.* **1978**, *69*, 1473.
(8) Lobaugh, J.; Voth, G. A. *J. Chem. Phys.* **1996**, *104*, 2056.
(9) Pavese, M.; Lu, S. D.; Lobaugh, J.; Voth, G. A. *J. Chem. Phys.* **1997**, *107*, 7428.
(10) Billeter, S. R.; van Gunsteren, W. F. *Comput. Phys. Commun*. **1997**, *107*, 61.
(11) Bicout, D.; Field, M., Eds. *Quantum mechanical simulation methods for studying biological systems;* Les Editions de Physique; Springer: Heidelberg and Les Ulis, 1996.
(12) Frisch, M. J.; Trucks, G. W.; Schlegel, H. B.; Gill, P. M. W.; Johnson, B. G.; Wong, M. W.; Foresman, J. B.; Robb, M. A.; Head-Gordon, M.; Replogle, E. S.; Gomperts, R.; Andres, J. L.; Raghavachari, K.; Binkley, J. S.; Gonzalez, C.; Martin, R. L.; Fox, D. J.; Defrees, D. J.; Baker, J.; Stewart, J. J. P.; Pople, J. A. *Gaussian 92/DFT,* Revision F.4; Gaussian, Inc.: Pittsburgh, PA 1993.
(13) Ando, K.; Hynes, J. T. *J. Mol. Liq.* **1995**, *64*, 25.
(14) Grigera, J. R.; Straatsma, T. P.; Berendsen, H. J. C. *J. Phys. Chem.* **1987**, *91*, 6269.
(15) van Gunsteren, W. F.; Billeter, S. R.; Eising, A. A.; Hünenberger, P. H.; Krüger, P.; Mark, A. E.; Scott, W. R. P.; Tironi, I. G. *Biomolecular Simulation: The GROMOS96 Manual and User Guide;* Biomos b.v. and, VdF Hochschulverlag, ETH Zürich: Zürich and Groningen, Zürich, 1996.
(16) Halle, B.; Karlström, G. *J. Chem. Soc., Faraday Trans. 2* **1983**, *79*, 1031.
(17) Halle, B.; Karlström, G. *J. Chem. Soc., Faraday Trans. 2* **1983**, *79*, 1047.
(18) Billeter, S. R.; van Gunsteren, W. F. *Mol. Simul.* **1995**, *15*, 301.